# Solid-State Characterization of Reduced Silver Vanadium Oxide from the Li/SVO Discharge Reaction

**Randolph A. Leising, William C. Thiebolt III, and Esther Sans Takeuchi***

Wilson Greatbatch Ltd., 10,000 Wehrle Drive, Clarence, New York 14031

*Received May 4, 1994*[⊗]

The reduction of silver vanadium oxide (SVO, $AgV_2O_{5.5}$) by lithium was studied via the solid-state characterization of the reduced cathode material. $Li_xAgV_2O_{5.5}$ products were isolated over a range of $0 < x < 3.3$, with corresponding voltages vs Li ranging from +3.25 to +1.8 V. X-ray powder diffraction analysis showed that the SVO materials lose crystallinity over the range $0 < x < 1.2$, with the simultaneous formation of elemental silver. In addition, the *c* lattice parameter for the samples decreased linearly from 7.56 to 6.55 Å over the range of $0 < x < 3.3$, indicating significant structural changes in the lithiated material. DSC and resistivity measurements also suggested structural changes in these products. The oxidation states of the vanadium and silver components were assigned on the basis of chemical analysis and X-ray powder diffraction results and were consistent with the results of FT-IR and room-temperature magnetic susceptibility measurements. Voltammetry of Li/SVO cells displayed multiple waves, which correlated with the results of the physical characterization studies. These experiments indicated that the reduction of SVO in lithium batteries can produce mixed-valent materials, with the presence of vanadium(V), -(IV) and -(III) possible in the same sample.

## Introduction

Characterization of the solid-state products of lithiation reactions can be challenging when the products are poorly crystalline or amorphous, limiting the use of X-ray crystallographic techniques. Further complications result when mixed-metal compounds are lithiated, since the reduction of these materials can result in a complex mixture of oxidation states. Nevertheless, these reactions are still of particular interest, since they occur during the discharge of solid-state cathode materials in lithium battery systems. The high-energy density offered by lithium batteries has made this technology highly desirable for new portable electronic devices as well as other applications where size and weight of the battery are critical.[1] One such lithium battery system uses silver vanadium oxide ($AgV_2O_{5.5}$, SVO) as a solid-state cathode.[2-4] The tunnel-like structure of SVO provides paths for the diffusion of lithium ions, and the high electrochemical potential of the material makes it a good candidate for this purpose. Indeed, SVO has been successfully used as a cathode material in lithium batteries for advanced biomedical devices such as the implantable cardiac defibrillator.[5] While the physical characterization of SVO starting material has been reported,[6-9] previous studies of the Li/SVO reaction have focused on the electrochemical characterization of the system.[10-12]

The study of the reduction products of SVO presents both difficulties described above. The Li/SVO reaction results in the reduction of $Ag^+$ to $Ag^0$ and $V^{5+}$ to $V^{4+}$ and $V^{3+}$, leading to a mixture of metal ions in a series of oxidation states at any given depth of discharge. In addition, utilizing a crystalline SVO starting material is not desirable, since highly crystalline forms of SVO have been shown to produce lower cell capacity.[7] Thus, the material of interest does not lend itself to complete characterization by crystal structure determination. This set of circumstances led us to examine a variety of solid-state characterization techniques to piece together a complete picture of the products of the Li/SVO reaction. We report here the physical characterization of solid-state SVO discharged in an electrochemical reaction with lithium using X-ray powder diffraction, DSC, FT-IR, room-temperature magnetic susceptibility and resistivity measurements. Wet chemical analysis was also conducted to confirm oxidation states of the samples. The results of the physical characterization experiments were correlated to the electrochemistry of the Li/SVO system.

## Experimental Section

The silver vanadium oxide starting material was synthesized for this study from a mixture of vanadium pentoxide with an aqueous solution of silver nitrate, using a ratio of silver to vanadium of 1:2. The mixture was brought to dryness and heated to a final temperature of 375 °C. The material was heated under an air atmosphere and ground at regular intervals throughout the synthesis to ensure adequate mixing of components.

**Caution!** *The decomposition of nitrate during SVO synthesis liberates $NO_x$ gas, which is highly toxic. This synthesis should be performed only in a well-ventilated fume hood.*

The electrochemical cell used to reduce SVO consisted of a single cathode combined with a lithium anode in 1M lithium hexafluoroarsenate in 50/50 by volume propylene carbonate/dimethoxyethane (PC/

[⊗] Abstract published in *Advance ACS Abstracts,* November 1, 1994.

(1) Nohma, T.; Yoshimura, S.; Nishio, K.; Saito, T. In *Lithium Batteries*; Pistoia, G., Ed.; Industrial Chemistry Library, Vol. 5; Elsevier: Amsterdam, 1994; Chapter 11.
(2) Liang, C. C.; Bolster, M. E.; Murphy, R. M. U.S. Patent 4 391 729, 1983.
(3) Liang, C. C.; Bolster, M. E.; Murphy, R. M. U.S. Patent 4 310 609, 1982.
(4) Takeuchi, E. S.; Thiebolt, W. In *Proceedings of the International Seminar on Lithium Battery Technology & Applications*, Deerfield Beach, FL, March 1991.
(5) Takeuchi, E. S. *Proceedings*, 6th Annual Battery Conference on Applications and Advances, Long Beach, CA, 1991; 91BM-1.
(6) Leising, R. A.; Takeuchi, E. S. *Chem. Mater.* **1993**, *5*, 738.
(7) Leising, R. A.; Takeuchi, E. S. *Chem. Mater.* **1994**, *6*, 489.
(8) Crespi, A. M.; Skarstad, P. M.; Zandbergen, H. W.; Schoonman, J. In *Proceedings of the Symposium on Lithium Batteries*; Surampudi, S., Koch, V. R., Eds.; The Electrochemical Society: Pennington, NJ, 1993; Vol. 93-24, p 98.
(9) Takeuchi, E. S.; Piliero, P. *J. Power Sources* **1987**, *21*, 133.
(10) Takeuchi, E. S.; Thiebolt, W. C. *J. Electrochem. Soc.* **1988**, *135*, 2691.
(11) Bergman, G. M.; Ebel, S. J.; Takeuchi, E. S.; Keister, P. *J. Power Sources* **1987**, *20*, 179.
(12) Takeuchi, E. S.; Thiebolt, W. C. *J. Electrochem. Soc.* **1991**, *138*, L44.

0020-1669/94/1333-5733$04.50/0 © 1994 American Chemical Society

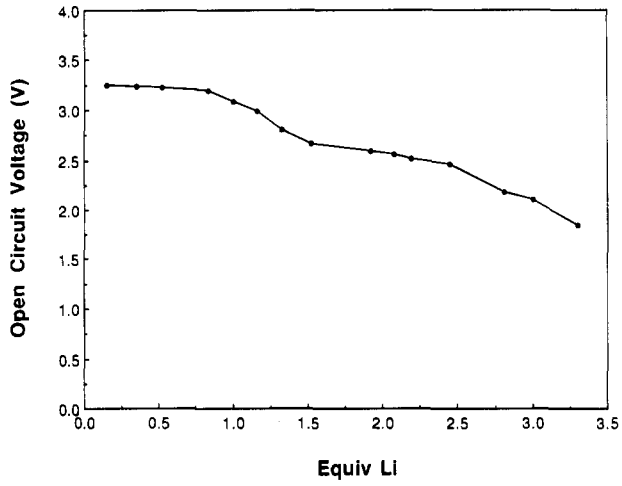


**Figure 1.** Constant resistance discharge curve for Li/SVO cells, where the voltage represents the final open circuit potential of the cells.

DME) electrolyte. Two layers of polypropylene microporous film were placed between the cathode and anode in the cell. The cathode consisted of a pellet containing 1.2 g of SVO, was pressed under a pressure of 0.54 kg/m$^2$, and sintered for 16 h at 375 °C. The cells were discharged under a constant (1000 Ω) resistance load at 25 °C in an inert atmosphere glovebox. The voltages of the cells were monitored during discharge using a linear strip-chart recorder. Resistivity measurements were performed on discharged SVO pellets which were taken directly from the electrochemical cells, washed with PC and DME solvents, and vacuum dried. The resistivity was measured via a linear four-point method[13] in an inert atmosphere glovebox. DSC, X-ray powder diffraction, magnetic susceptibility, FT-IR and chemical analysis experiments were all performed on samples ground with a mortar and pestle to produce a powder. Differential Scanning Calorimetry (DSC) analyses of the SVO samples were obtained using a DuPont Instruments TA 2000 DSC. The samples were analyzed under a purge of argon (120 mL/min) in hermetically sealed Al pans to 600 °C at a heating rate of 20 °C/min. X-ray powder diffraction spectra of discharged silver vanadium oxide samples were recorded on a Siemens Diffrac 500 instrument using Cu Kα radiation (1.540 56 Å). Spectra were recorded from 10 to 80° (2$\theta$). Si powder (99.999%, Aldrich Chemical) was used as an internal standard for the samples, where a weighed sample of Si was thoroughly mixed with a known amount of SVO. The amount of Si standard was 4% (wt %) of the entire sample. The samples were kept under an inert atmosphere until data were collected. Exposing the X-ray samples to an air atmosphere briefly during the experiment did not appear to alter the materials since DSC curves of the samples analyzed by XRPD were identical to those found for the samples prior to the experiment. Magnetic susceptibilities of powdered samples were measured using a Johnson Matthey magnetic susceptibility balance at 25 °C in a dry atmosphere. FT-IR diffuse reflectance spectra of the discharged SVO samples were recorded with a Mattson Cygnus 100 spectrometer. Chemical analysis of the SVO samples dissolved in sulfuric acid was performed via a combination of potassium permanganate titrations and sulfur dioxide reduction of the vanadium components of the materials.[10]

## Results and Discussion

Lithium/silver vanadium oxide electrochemical cells containing nonaqueous electrolyte were discharged under constant resistive loads to different voltage limits. The coulometric titration curve[14] for the Li/SVO system is illustrated in Figure 1, where the final voltages (open circuit potentials) of the discharged test cells were plotted as a function of the equiv of Li incorporated into the cathode. Each point in Figure 1 represents a separate cell, which was disassembled following discharge and from which the cathode material was isolated. The average voltage during discharge and final open circuit voltage for each Li/SVO cell are listed in Table 1. The capacity removed from the cell is also given in Table 1, and is calculated on the basis of the average cell voltage, resistive load, and time on load using Ohm's law.

The SVO starting material used in this study was analyzed by X-ray powder diffraction (XRPD). The powder pattern for this material is displayed in Figure 2, and is consistent with a poorly crystalline sample, displaying low signal intensities and broad lines. The material was chosen for this study over more crystalline forms of $AgV_2O_{5.5}$ since it displays higher capacity and pulse power capability than the highly crystalline species.[7] However, this less crystalline material gives rise to the same *d*-spacings as seen in the pattern reported in the literature for $\epsilon$-phase $Ag_2V_4O_{11}$[15] (Table 2), indicating the same structure for the materials. In addition, the X-ray pattern for this sample was indexed using the monoclinic unit cell parameters $a = 15.33$ Å, $b = 3.587$ Å, $c = 9.526$ Å, and $\beta = 127.9°$ taken from ref 8. The Miller indices for these peaks are listed in Table 2, and match the indices listed for $Ag_2V_4O_{11}$ in the reference. In that study a structure was proposed consisting of layers of $V_4O_{11}$ with silver between the layers. Layered structures are typically unstable for simple metal oxides, but are stabilized by the insertion of large cations (such as $Ag^+$) between the layers.[16] For the unit cell of SVO the $V_4O_{11}$ layers are positioned in the plane formed by the *a*- and *c*-axes, with the *b*-axis representing the distance between the layers.[8]

The discharged SVO samples were also analyzed by XRPD, and the results are summarized in Table 3. The discharge reaction produces two obvious changes in the X-ray patterns: (1) a decrease in intensity of SVO peaks with increasing discharge and (2) the appearance of absorbances due to silver metal. The loss of crystalline SVO is evident from the decrease in intensity of the SVO peaks (Table 3), where these peaks have completely disappeared by the time 1.2 equiv of Li has been incorporated into the sample. This suggests that the SVO cathode material becomes nearly amorphous with the incorporation of lithium. A loss in crystallinity with lithiation has also been observed for copper vanadates, $CuV_2O_6$[17] and $\alpha$-$Cu_2V_2O_7$.[18] The rise in peaks due to silver metal in discharged SVO can be seen in $Li_{0.35}AgV_2O_{5.5}$ and $Li_{0.5}AgV_2O_{5.5}$ in Figure 2, with the peak at 2.36 Å (38.1° 2$\theta$) displaying the greatest intensity. These lines are more obvious in Figure 3 for $Li_{3.0}AgV_2O_{5.5}$ (Si standard is omitted from this sample), with *d*-spacings of 2.36 Å (111), 2.04 Å (200), 1.44 Å (220) and 1.23 Å (311) corresponding to silver. The amount of reduced silver in the samples was quantified using a Si internal standard,[19] and is tabulated in Table 3. Figure 4 displays a plot of the amount of reduced silver as a function of Li equiv, and shows a nearly linear increase in silver metal as the samples are discharged from 0 to 1.2 equiv of Li. It should be noted that significant experimental error (~10−15%) is expected in quantifying the amount of silver by this technique, due to the poorly crystalline nature of these samples. The silver metal peaks display significant line broadening, with peak widths at half-height ($W_{1/2}$) in the range 0.7−1.0° (2$\theta$) for the 111 peak of Ag. By comparison, mixtures of unreacted SVO with 5 $\mu$ silver powder displayed $W_{1/2}$ values

(13) Runyan, W. R. *Semiconductor Measurements and Instrumentation*; McGraw-Hill: New York, 1976; p 69.
(14) Wagner, C. *J. Chem. Phys.* **1953**, *21*, 1819.
(15) Raveau, B. *Rev. Chim. Miner.* **1967**, *4*, 729.
(16) Delmas, C. In *Lithium Batteries*; Pistoia, G., Ed.; Industrial Chemistry Library, Vol. 5; Elsevier: Amsterdam, 1994; Chapter 12.
(17) Sakurai, Y.; Ohtsuka, H.; Yamaki, J.-I. *J. Electrochem. Soc.* **1988**, *135*, 32.
(18) Ilic, D.; Neumann, D. *J. Power Sources* **1993**, *43*−*44*, 589.
(19) Klug, H. P.; Alexander, L. E. *X-Ray Diffraction Procedures*, 2nd ed.; Wiley-Interscience: New York, 1974; p 536.

**Table 1.** Discharge Results and Empirical Formulas for Lithiated SVO Samples

| capacity removed (mA h)[a] | av voltage (V)[b] | open circuit voltage (V)[c] | equiv of Li[d] | formula[e] |
|---|---|---|---|---|
| 10.8 | 2.840 | 3.243 | 0.15 | $Li_{0.15}Ag^{+}_{0.9}Ag^{0}_{0.1}V^{5+}_{1.95}V^{4+}_{0.05}V^{3+}_{0.0}O_{5.5}$ |
| 31.9 | 2.869 | 3.234 | 0.35 | $Li_{0.35}Ag^{+}_{0.8}Ag^{0}_{0.2}V^{5+}_{1.9}V^{4+}_{0.1}V^{3+}_{0.0}O_{5.5}$ |
| 53.2 | 2.842 | 3.231 | 0.52 | $Li_{0.5}Ag^{+}_{0.6}Ag^{0}_{0.4}V^{5+}_{1.9}V^{4+}_{0.1}V^{3+}_{0.0}O_{5.5}$ |
| 84.9 | 2.801 | 3.197 | 0.83 | $Li_{0.8}Ag^{+}_{0.4}Ag^{0}_{0.6}V^{5+}_{1.8}V^{4+}_{0.2}V^{3+}_{0.0}O_{5.5}$ |
| 107.9 | 2.770 | 3.090 | 1.00 | $Li_{1.0}Ag^{+}_{0.3}Ag^{0}_{0.7}V^{5+}_{1.7}V^{4+}_{0.3}V^{3+}_{0.0}O_{5.5}$ |
| 127.2 | 2.741 | 2.991 | 1.16 | $Li_{1.2}Ag^{+}_{0.1}Ag^{0}_{0.9}V^{5+}_{1.7}V^{4+}_{0.3}V^{3+}_{0.0}O_{5.5}$ |
| 146.7 | 2.706 | 2.809 | 1.32 | $Li_{1.3}Ag^{+}_{0.1}Ag^{0}_{0.9}V^{5+}_{1.6}V^{4+}_{0.4}V^{3+}_{0.0}O_{5.5}$ |
| 170.1 | 2.678 | 2.667 | 1.52 | $Li_{1.5}Ag^{+}_{0.0}Ag^{0}_{1.0}V^{5+}_{1.5}V^{4+}_{0.5}V^{3+}_{0.0}O_{5.5}$ |
| 212.4 | 2.625 | 2.595 | 1.92 | $Li_{1.9}Ag^{+}_{0.0}Ag^{0}_{1.0}V^{5+}_{1.1}V^{4+}_{0.9}V^{3+}_{0.01}O_{5.5}$ |
| 235.5 | 2.600 | 2.558 | 2.08 | $Li_{2.1}Ag^{+}_{0.0}Ag^{0}_{1.0}V^{5+}_{0.9}V^{4+}_{1.0}V^{3+}_{0.02}O_{5.5}$ |
| 256.1 | 2.571 | 2.519 | 2.19 | $Li_{2.2}Ag^{+}_{0.0}Ag^{0}_{1.0}V^{5+}_{0.8}V^{4+}_{1.15}V^{3+}_{0.05}O_{5.5}$ |
| 279.9 | 2.542 | 2.460 | 2.45 | $Li_{2.4}Ag^{+}_{0.0}Ag^{0}_{1.0}V^{5+}_{0.6}V^{4+}_{1.35}V^{3+}_{0.05}O_{5.5}$ |
| 320.5 | 2.467 | 2.187 | 2.81 | $Li_{2.8}Ag^{+}_{0.0}Ag^{0}_{1.0}V^{5+}_{0.2}V^{4+}_{1.75}V^{3+}_{0.05}O_{5.5}$ |
| 345.1 | 2.416 | 2.109 | 3.00 | $Li_{3.0}Ag^{+}_{0.0}Ag^{0}_{0.9}V^{5+}_{0.1}V^{4+}_{1.7}V^{3+}_{0.2}O_{5.5}$ |
| 379.6 | 2.200 | 1.849 | 3.30 | $Li_{3.3}Ag^{+}_{0.0}Ag^{0}_{0.9}V^{5+}_{0.0}V^{4+}_{1.6}V^{3+}_{0.4}O_{5.5}$ |

[a] Capacity calculated on the basis of (average voltage/1000 Ω) × time on load. [b] Average voltage during discharge of cell at 25 °C under 1000 Ω load. [c] Final open circuit voltage for cell allowed to equilibrate at open circuit for 7−21 days. [d] Equivalents of Li assigned on the basis of permanganate titration. [e] Formula assigned on the basis of permanganate titration and X-ray powder diffraction results.

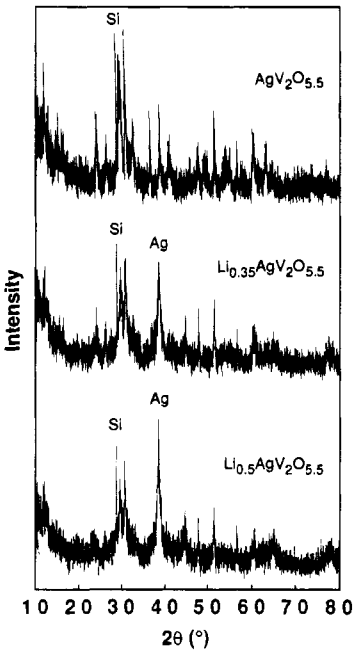


**Figure 2.** X-ray powder diffraction patterns of SVO and discharged SVO samples recorded using Cu Kα radiation. Si powder was added as an internal standard. Ag designates the absorbances assigned to silver metal.

**Table 2.** X-ray Powder Diffraction Peaks (*d*-Spacings, Intensities) for SVO Starting Material

| $d_{obs}$ (Å) | int | $d_{lit.}$ (Å)[a] | int | $d_{calc}$ (Å)[b] | Miller indices (*hkl*)[b] |
|---|---|---|---|---|---|
| 7.56 | 40 | 7.50 | 60 | 7.52 | 001 |
| 5.94 | 30 | | | 6.05 | 200 |
| 3.82 | 50 | 3.75 | 70 | 3.76 | 002 |
| 3.75 | 40 | 3.71 | 30 | 3.73 | 201 |
| 3.45 | 30 | 3.43 | 70 | 3.44 | $1\bar{1}0$ |
| 3.06 | 100 | 3.08 | 70 | 3.08 | $\bar{2}03$ |
| 3.01 | 70 | 3.00 | 60 | 3.02 | 400 |
| 2.93 | 80 | 2.92 | 100 | 2.94 | $1\bar{1}1$ |
| 2.79 | 40 | 2.77 | 80 | 2.79 | $\bar{1}12$ |
| | | 2.66 | 40 | 2.68 | $3\bar{1}0$ |
| 2.49 | 40 | 2.46 | 40 | 2.48 | $\bar{6}03$ |
| 2.34 | 50 | 2.32 | 70 | 2.31 | 410 |
| 2.23 | 40 | 2.20 | 60 | 2.20 | 103 |
| 1.97 | 20 | 1.99 | 10 | 2.01 | $5\bar{1}0$ |
| 1.92 | 20 | 1.96 | 10 | 1.96 | $\bar{3}14$ |
| 1.87 | 20 | 1.86 | 40 | 1.86 | $40\bar{2}$ |
| | | 1.83 | 10 | 1.82 | $30\bar{5}$ |
| 1.79 | 50 | 1.78 | 70 | 1.77 | 120 |
| 1.71 | 30 | 1.70 | 40 | 1.70 | 104 |
| 1.69 | 20 | 1.67 | 60 | 1.67 | $41\bar{5}$ |
| 1.63 | 20 | 1.60 | 30 | 1.60 | $90\bar{5}$ |
| 1.54 | 30 | 1.54 | 70 | 1.54 | 114 |
| 1.48 | 30 | 1.47 | 60 | 1.47 | 222 |

[a] Reference 15. [b] Pattern indexed using the unit cell parameters $a$ = 15.33 Å, $b$ = 3.587 Å, $c$ = 9.526 Å, and $\beta$ = 127.9° from ref 8.

of 0.2° for the same Ag peak under these conditions. This suggests that the reduced silver is disordered in the lithiated SVO samples. The formation of silver(0) in these samples is reminiscent of the reduction of copper vanadates, which results in the formation of elemental copper.[17]

Upon closer examination of the X-ray powder patterns for the discharged SVO samples, another change is evident. The 001 peak of SVO is present in all of the patterns, even though the other SVO peaks disappear at $x \geq 1.2$. This can be seen in Figure 3 for $Li_{3.0}AgV_2O_{5.5}$, where only the peaks corresponding to silver metal and the SVO 001 peak remain. This is reminiscent of XRPD results for the lithiation of $Nb_2O_5$, where the intensity of the 001 peak was constant while the other peaks decreased in intensity with discharge.[20] The ratio of peak intensities $I/I_{001}$ was used in that study to estimate disorder in the lithiated material. However, unlike the $Nb_2O_5$ system which maintains a constant *d*-spacing for the 001 peak during discharge, the lithiated SVO samples display a shift in *d*-spacing for the 001 line. The *d*-spacings for these peaks are listed in Table 3, and show that the spacing between the *c*-planes decreases with increasing incorporation of lithium, from 7.56 Å for starting SVO down to 6.55 Å for $Li_{3.0}AgV_2O_{5.5}$. This corresponds to a 13% contraction in the *c* lattice parameter of the unit cell. A contraction of the *c*-axis is notable, since the cathode materials were found to swell during the discharge reaction by 28% from $AgV_2O_{5.5}$ to $Li_{3.0}AgV_2O_{5.5}$. This is based on cathode volumes of the pressed pellet electrodes measured after the discharge reaction, which are listed in Table 3. This suggests that while the *c* lattice parameter becomes smaller, the *a* and/or *b* parameters become larger, along with a possible change in $\beta$. A change in unit cell parameters was noted in the X-ray diffraction patterns for lithiated vanadium oxide, where the phase transition from $Li_{1.2}V_3O_8$ to rock salt $Li_{4.0}V_3O_8$ was accompanied by a contraction of the *a* lattice parameter, and

(20) Kumagai, N.; Tanno, K.; Nakajima, T.; Watanabe, N. *Electrochim. Acta* **1983**, *28*, 17.

**Table 3.** X-ray Powder Diffraction Results for Discharged SVO Samples

| sample | % $Ag^0$ metal[a] | % SVO[b] | $d_{001}$ (Å)[c] | cathode vol $(cm^3)$[d] |
|---|---|---|---|---|
| $AgV_2O_{5.5}$ | 0 | 100 | 7.56 | 0.334 |
| $Li_{0.15}AgV_2O_{5.5}$ | 10 | 90 | 7.45 | 0.346 |
| $Li_{0.35}AgV_2O_{5.5}$ | 25 | 70 | 7.39 | 0.354 |
| $Li_{0.5}AgV_2O_{5.5}$ | 40 | 50 | 7.38 | 0.364 |
| $Li_{0.8}AgV_2O_{5.5}$ | 60 | 10 | 7.28 | 0.371 |
| $Li_{1.2}AgV_2O_{5.5}$ | 90 | 0 | 7.10 | 0.386 |
| $Li_{1.5}AgV_2O_{5.5}$ | 95 | 0 | 6.96 | |
| $Li_{2.1}AgV_2O_{5.5}$ | 95 | 0 | 6.89 | 0.412 |
| $Li_{3.0}AgV_2O_{5.5}$ | 90 | 0 | 6.55 | 0.426 |

[a] Percent of silver metal based on total silver content in sample. [b] Percent of crystalline SVO in powder pattern based on amount of starting SVO. [c] $d_{001}$ peak assigned using unit cell parameters $a = 15.33$ Å, $b = 3.587$ Å, $c = 9.526$ Å, $\beta = 127.9°$.[9] [d] Volume of cathode pellet taken from the discharged cell.

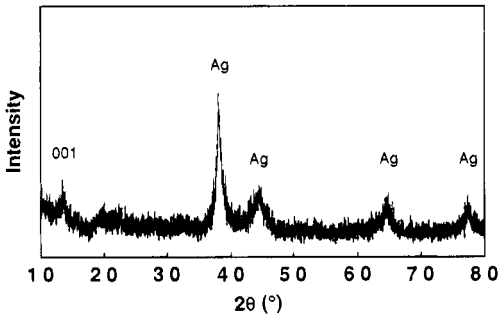


**Figure 3.** X-ray powder diffraction pattern of $Li_{3.0}AgV_2O_{5.5}$ recorded using Cu Kα radiation. The 001 line of the discharged SVO is identified along with peaks assigned to silver metal.

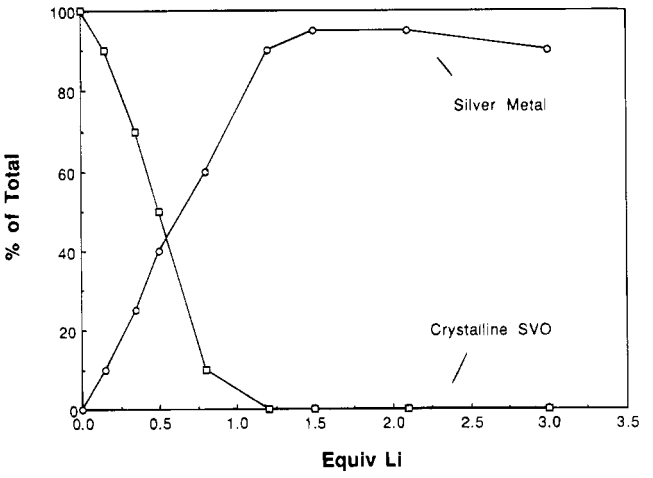


**Figure 4.** Percent of silver metal and crystalline SVO observed in the X-ray powder diffraction patterns for the discharged SVO samples. Percent values are based on total silver and crystalline SVO in the starting material.

expansion of the *b* and *c* parameters.[21] Contraction of the *a* parameter coupled with expansion of the *c* parameter was also observed in the lithiation of orthorhombic $V_2O_5$ in the range of $0.2 < x < 0.7$ for $Li_xV_2O_5$,[22] along with a 13% expansion along the *b*-axis for $x = 1$.[20] Likewise, the removal (deintercalation) of lithium from $\gamma$-$LiV_2O_5$ bronze causes a decrease in the *c* parameter and increase in the *a* parameter for this species.[23] It should be noted that the orthorhombic unit cell parameters for the vanadium oxides correspond to different structural features than the monoclinic lattice parameters for SVO. For example, in $\gamma$-$LiV_2O_5$ the *c* parameter is equal to twice the distance between the vanadium oxide layers, while the *a* parameter represents the distance between vanadium oxide ribbons.[23] Considering the structure of SVO described above, the orthorhombic *c* and *a* parameters of $LiV_2O_5$ correspond to the SVO unit cell parameters of $b(\times 2)$ and *c*, respectively.

Chemical analysis via permanganate titration of the SVO reaction products dissolved in sulfuric acid solution was used to confirm the depth of discharge of the materials. Analyses of this type have been previously used to provide information on the oxidation states of the vanadium components of discharged SVO.[10] By combining permanganate titration with $SO_2$ reduction of SVO samples, the relative amounts of $V^{5+}$, $V^{4+}$, and $V^{3+}$ in solution can be determined. However, in this study we determined that samples containing $V^{5+}$ and $Ag^0$ will react when dissolved to give $V^{4+}$ and $Ag^+$, according to eq 1.

$$V^{5+} + Ag^0 \rightarrow V^{4+} + Ag^+ \quad (1)$$

Thus, the amount of silver(I) in the dissolved samples will be greater than in the corresponding solid-state material, unless all of the vanadium(V) has already been reduced in the solid-state. By the same token, the amount of vanadium(V) will be lower in the dissolved sample. This complicates the correlation between the solid-state and solution analyses, and is reflected in Tables 1 and 2 of ref 10, where the percent of silver present as silver(0) was listed as zero until all of the vanadium(V) was gone. To eliminate this complication, the X-ray powder diffraction results were used in the present study to determine the amount of elemental silver in samples containing vanadium-(V). The final ratios of oxidation states are listed in Table 1 in the formulas assigned to the discharged species. These formulas are an estimate of the composition of the solid-state materials taking into account the effect of the reaction in eq 1 on the ratio of vanadium oxidation states determined by chemical analysis. Interestingly, in this study vanadium(V) was found to exist along with vanadium(III) in the solid-state materials, indicating that some vanadium(IV) is reduced before vanadium-(V) in the samples.

The bulk magnetic susceptibilities of the powdered discharged samples were measured at room temperature. The molar susceptibility values ($\chi_m$) are listed in Table 4 along with expected values calculated based on the summation of the individual susceptibilities of each species present in the sample. The susceptibility factors used in the calculations for $V^{3+}$, $V^{4+}$, and $V^{5+}$ are based on the room-temperature susceptibilities of $V_2O_3$, $VO_2$, and $V_2O_5$, respectively.[24] In addition, the magnetic susceptibility for $Ag^0$ was also used in the calculation, along with diamagnetic corrections for $Li^+$ and $Ag^+$. A comparison of observed and calculated molar susceptibilities for the lithiated SVO samples is plotted in Figure 5 as a function of depth of discharge. The experimental data are similar to the calculated susceptibilities, consistent with the formulations assigned to the discharged species by X-ray powder diffraction and chemical analysis. Interestingly, the susceptibility curves are relatively flat up to a depth of discharge corresponding to ~1.2 equiv of lithium, where a large increase in slope takes place. This change in slope can be explained by a shift in reduction from primarily silver to vanadium, since the susceptibility of $Ag^0$ is much smaller than that of $V^{4+}$ or $V^{3+}$. In the range of $0 < x < 1.2$ for $Li_xAgV_2O_{5.5}$ silver reduction dominates, resulting in only

(21) de Picciotto, L. A.; Adendorff, K. T.; Liles, D. C.; Thackeray, M. M. *Solid State Ionics* **1993**, *62*, 297.
(22) Hub, S.; Tranchant, A.; Messina, R. *Electrochim. Acta* **1988**, *33*, 997.
(23) Cocciantelli, J. M.; Menetrier, M.; Delmas, C.; Doumerc, J. P.; Pouchard, M.; Hagenmuller, P. *Solid State Ionics* **1992**, *50*, 99.
(24) Weast, R. C., Ed. *CRC Handbook of Chemistry and Physics*, 61st ed.; CRC Press: Boca Raton, FL, 1980; p E127.

**Table 4.** Magnetic Susceptibilities for Discharged SVO Samples[a]

| sample | $\chi_m^{obs}$ ($10^6$ cgsu) | $\chi_m^{calc}$ ($10^6$ cgsu) | sample | $\chi_m^{obs}$ ($10^6$ cgsu) | $\chi_m^{calc}$ ($10^6$ cgsu) |
|---|---|---|---|---|---|
| $Li_{0.15}AgV_2O_{5.5}$ | 147 | 224 | $Li_{1.9}AgV_2O_{5.5}$ | 911 | 706 |
| $Li_{0.35}AgV_2O_{5.5}$ | 258 | 278 | $Li_{2.1}AgV_2O_{5.5}$ | 1024 | 815 |
| $Li_{0.5}AgV_2O_{5.5}$ | 283 | 214 | $Li_{2.2}AgV_2O_{5.5}$ | 1165 | 958 |
| $Li_{0.8}AgV_2O_{5.5}$ | 358 | 254 | $Li_{2.4}AgV_2O_{5.5}$ | 1040 | 1105 |
| $Li_{1.2}AgV_2O_{5.5}$ | 343 | 215 | $Li_{2.8}AgV_2O_{5.5}$ | 1362 | 1423 |
| $Li_{1.3}AgV_2O_{5.5}$ | 789 | 334 | $Li_{3.0}AgV_2O_{5.5}$ | 1518 | 1658 |
| $Li_{1.5}AgV_2O_{5.5}$ | 564 | 388 | $Li_{3.3}AgV_2O_{5.5}$ | 1629 | 1926 |

[a] Magnetic susceptibilities were determined at 25 °C on powdered samples.

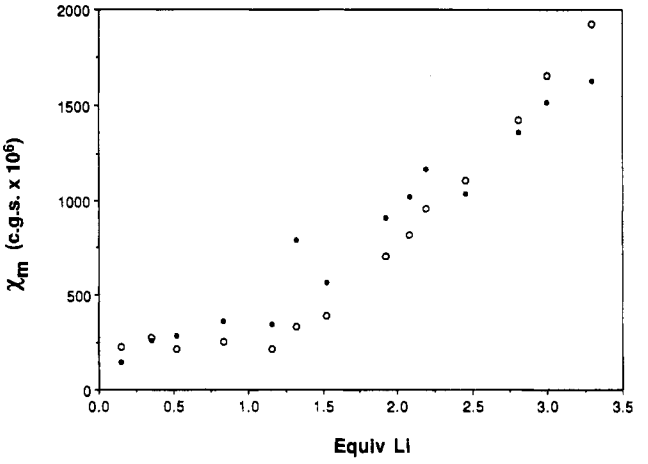


**Figure 5.** Room-temperature magnetic susceptibility of powdered samples of discharged SVO: (○) calculated molar susceptibility; (●) observed molar susceptibility.

**Table 5.** Resistivity of Discharged SVO Samples

| sample | resistivity (Ω·cm) | sample | resistivity (Ω·cm) |
|---|---|---|---|
| $AgV_2O_{5.5}$ | 330 | $Li_{0.8}AgV_2O_{5.5}$ | $1.5 \times 10^{-3}$ |
| $Li_{0.04}AgV_2O_{5.5}$ | 25 | $Li_{1.0}AgV_2O_{5.5}$ | $1.2 \times 10^{-3}$ |
| $Li_{0.15}AgV_2O_{5.5}$ | $3.4 \times 10^{-2}$ | $Li_{1.9}AgV_2O_{5.5}$ | $1.7 \times 10^{-3}$ |
| $Li_{0.35}AgV_2O_{5.5}$ | $2.6 \times 10^{-3}$ | $Li_{2.8}AgV_2O_{5.5}$ | $5.8 \times 10^{-3}$ |
| $Li_{0.5}AgV_2O_{5.5}$ | $1.8 \times 10^{-3}$ | $Li_{3.3}AgV_2O_{5.5}$ | $4.0 \times 10^{-2}$ |

very small increases in susceptibility. In the range of $1.2 < x < 3.3$, reduction of vanadium takes place, rapidly increasing the susceptibility of the sample.

The conductivity of discharged SVO was analyzed via resistivity measurements of cathode plates taken directly from the electrochemical cells. The results are presented in Table 5 and show that the unreacted SVO has a resistivity of 330 Ω·cm. It should be noted that resistivity measurements of this type can vary depending on grain boundaries in the pressed plates,[13] so that these measurements were used only to identify trends in the data. The addition of 0.4 equiv of Li resulted in a decrease in resistivity of over 5 orders of magnitude to $2.6 \times 10^{-3}$ Ω·cm. Some of the decrease in resistance may be attributed to the formation of conductive elemental silver in the samples, as identified in the X-ray powder diffraction analysis. However, a study of pressed plates of SVO containing silver metal powder showed that a sample with 0.4 equiv of $Ag^0$ displayed a resistivity only tenfold lower than the starting material. Thus, the large decrease in resistivity must also depend on the change in structure accompanying the discharge of the samples. A similar change in electronic conductivity was identified for $Fe_2O_3$, where the addition of 1 equiv of Li to α-$Fe_2O_3$ resulted in a drop in resistivity from $10^{12}$ to 19 Ω·cm.[25] The resistivity of the $Li_xAgV_2O_{5.5}$ reaches a minimum at $x \sim 1$, and then increases slightly with the introduction of more lithium into the sample (Table 5). An important consequence of the high electronic conductivity of the lithiated SVO is that electrodes can be fabricated from SVO without the need for large amounts of conductive additives.

The thermal properties of the lithiated SVO products were analyzed using differential scanning calorimetry (DSC). The results are tabulated in Table 6, and representative curves are displayed in Figure 6. The assignment of the transitions in the DSC curve for nondischarged SVO have been discussed previously.[6,7] The sharp endothermic transitions at 537 and 552 °C are most likely due to a peritectic transformation (527 °C) and eutectic point (545 °C) of $AgV_2O_{5.5}$, and the exothermic peak at 562 °C may be caused by a crystalline phase change in the material. The melting point of $AgV_2O_{5.5}$ is ~640 °C, which is beyond the 600 °C limit of the experiment. The $Li_xAgV_2O_{5.5}$ materials display DSC curves very different from the starting material. For $0 < x < 1.2$ the samples produced DSC curves containing sharp endotherms in the temperature range of 465–565 °C. This is similar to the major isotherms observed for the starting material. Between 1.2 and 1.9 equiv of Li sharp exotherms are observed in the DSC curves in the temperature range ~200–350 °C, while the endothermic transitions have disappeared. The loss of sharp endotherms from the DSC curves occurs at the transition from primarily silver reduction to vanadium(V) reduction in the reaction. This suggests that a significant phase change takes place with the reduction of the bulk $V^{5+}$ to $V^{4+}$. Finally, between 1.9 and 3.3 equiv of Li relatively featureless DSC curves are observed. The melting point of silver metal (962 °C) produced in these samples is beyond the limit of the experiment.

The diffuse reflectance FT-IR spectra were analyzed for the solid-state lithiated samples diluted with KBr. The results are presented in Table 7 and representative spectra are illustrated in Figure 7. The infrared spectra of alkaline metavanadates have been assigned in the literature, and these assignments are useful in elucidating the spectra of the SVO starting material. Bands between 960 and 875 $cm^{-1}$ were reported to correspond to the symmetric and antisymmetric stretching modes of V=O bonds.[26] In addition, strong bands between 860 and 835 $cm^{-1}$ were assigned to the antisymmetric stretching of V–O–V, and the peaks in the 700–470 $cm^{-1}$ region were due to bending and symmetric stretching modes of the V–O–V bonds. Likewise, in $V_2O_5$ a sharp band at 1029 $cm^{-1}$ is assigned to the $V^{5+}$=O stretching frequency, and broad bands at 835 and 606 $cm^{-1}$ are assigned to the antisymmetric and symmetric stretching modes for V–O–V, respectively.[27] In comparison, the addition of silver to the vanadium oxide matrix found in $AgV_2O_{5.5}$ resulted in a red shift for the $V^{5+}$=O stretching frequencies to 984–932 $cm^{-1}$ (Figure 7). This red shift has been explained as resulting from a weakening of the V=O bond, due to interaction between $Ag^+$ and the unbridged oxygen atoms of the vanadium

(25) Abraham, K. M.; Pasquariello, D. M.; Willstaedt, E. B. *J. Electrochem. Soc.* **1990**, *137*, 743.
(26) Dimitriev, Y.; Dimitrov, V.; Arnaudov, M. *J. Mater. Sci.* **1979**, *14*, 723.
(27) Frederickson, L. D.; Hausen, D. M. *Anal. Chem.* **1963**, *35*, 818.

**Table 6.** Differential Scanning Calorimetry Isotherms for Discharged SVO Samples

| sample | isotherms[a] (°C) |
|---|---|
| $AgV_2O_{5.5}$ | 463 (endo), 537 (endo), 552 (endo), 562 (exo) |
| $Li_{0.04}AgV_2O_{5.5}$ | 415 (exo), 531 (endo), 552 (endo), 563 (exo) |
| $Li_{0.15}AgV_2O_{5.5}$ | 187 (exo), 214 (exo), 324 (exo), 400 (exo), 489 (endo), 516 (endo) |
| $Li_{0.35}AgV_2O_{5.5}$ | 188 (exo), 221 (exo), 313 (exo), 399 (exo), 470 (endo), 479 (endo) |
| $Li_{0.5}AgV_2O_{5.5}$ | 186 (exo), 212 (exo), 308 (exo), 391 (exo), 469 (endo), 481 (endo), 510 (endo) |
| $Li_{0.8}AgV_2O_{5.5}$ | 189 (exo), 212 (exo), 312 (exo), 321 (exo), 370 (exo), 466 (endo), 502 (endo), 506 (endo) |
| $Li_{1.2}AgV_2O_{5.5}$ | 217 (exo), 248 (exo), 281 (exo), 500 (endo), 558 (endo) |
| $Li_{1.3}AgV_2O_{5.5}$ | 143 (exo), 220 (exo), 249 (exo) |
| $Li_{1.5}AgV_2O_{5.5}$ | 111 (exo), 209 (exo), 260 (exo), 289 (exo) |
| $Li_{1.9}AgV_2O_{5.5}$ | 114 (exo), 206 (exo), 309 (exo), 442 (exo), 496 (exo) |
| $Li_{2.1}AgV_2O_{5.5}$ | 110 (exo), 212 (exo), 313 (endo), 450 (exo), 500 (exo) |
| $Li_{2.2}AgV_2O_{5.5}$ | 91 (exo), 212 (exo), 313 (endo), 457 (exo) |
| $Li_{2.4}AgV_2O_{5.5}$ | 106 (exo), 216 (exo), 242 (exo), 292 (endo), 321 (endo), 465 (exo) |
| $Li_{2.8}AgV_2O_{5.5}$ | 88 (exo), 213 (exo), 246 (exo), 336 (endo), 493 (exo) |
| $Li_{3.0}AgV_2O_{5.5}$ | 78 (exo), 216 (exo), 250 (exo), 336 (endo), 413 (endo), 520 (exo) |
| $Li_{3.3}AgV_2O_{5.5}$ | 78 (exo), 210 (exo), 272 (exo), 445 (endo) |

[a] Endo = endothermic peak; exo = exothermic peak.

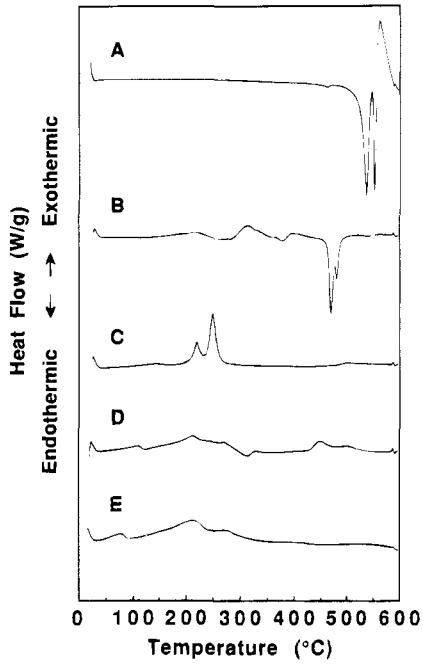


**Figure 6.** Differential scanning calorimetry curves for SVO and discharged SVO samples measured under a purge of Ar gas. A heating rate of 20 °C/min and an argon purge rate of 120 mL/min were employed for the analysis: (A) $AgV_2O_{5.5}$; (B) $Li_{0.35}AgV_2O_{5.5}$; (C) $Li_{1.3}AgV_2O_{5.5}$; (D) $Li_{2.1}AgV_2O_{5.5}$; (E) $Li_{3.3}AgV_2O_{5.5}$.

oxide lattice.[28,29] Finally, the splitting of the V=O band into a multiplet as seen here is also observed for $V_2O_5$ doped with heavy alkali metals.[30]

The reduction of the SVO material is accompanied by a change in intensity and position of the infrared bands observed for the starting material. Just as the intensity of the V−O−V bands are decreased for $VO_2$ relative to $V_2O_5$,[27] the bands at 870, 746, and 583 $cm^{-1}$ decrease in intensity with the reduction of $AgV_2O_{5.5}$ (Figure 7). By the time 1.2 equiv of Li is incorporated into SVO, these low-frequency bands have disappeared completely. Interestingly, the absorptions assigned to V=O stretching display a blue shift for these samples, shifting from 932 to 961 $cm^{-1}$ for the largest peak. This shift in wavenumber is consistent with the reduction of $Ag^+$ to $Ag^0$,

**Table 7.** FT-IR Spectral Data for Discharged SVO Samples[a]

| sample | wavenumber ($cm^{-1}$) | | | | | |
|---|---|---|---|---|---|---|
| $AgV_2O_{5.5}$ | 984 | 966 | 932 | 870 | 746 | 583 |
| $Li_{0.04}AgV_2O_{5.5}$ | 984 | 964 | 930 | 870 | 725 | 588 |
| $Li_{0.15}AgV_2O_{5.5}$ | 980 | 961 | 930 | 864 | 704 | 590 |
| $Li_{0.35}AgV_2O_{5.5}$ | 999 | 957 | 932 | 800 | 710 | 588 |
| $Li_{0.5}AgV_2O_{5.5}$ | 997 | | 943 | | 716 | |
| $Li_{0.8}AgV_2O_{5.5}$ | 995 | | 959 | | 705 | |
| $Li_{1.2}AgV_2O_{5.5}$ | 997 | | 961 | | 713 | |
| $Li_{1.3}AgV_2O_{5.5}$ | 997 | | 957 | | 714 | |
| $Li_{1.5}AgV_2O_{5.5}$ | 991 | | 951 | | 711 | |
| $Li_{1.9}AgV_2O_{5.5}$ | 988 | | 936 | | 714 | |
| $Li_{2.1}AgV_2O_{5.5}$ | 986 | | 928 | | 716 | |
| $Li_{2.2}AgV_2O_{5.5}$ | | | 924 | | 716 | 592 |
| $Li_{2.4}AgV_2O_{5.5}$ | | | 916 | | 714 | 590 |
| $Li_{2.8}AgV_2O_{5.5}$ | | | 904 | 878 | 712 | 590 |
| $Li_{3.0}AgV_2O_{5.5}$ | | | 899 | 874 | 706 | 590 |
| $Li_{3.3}AgV_2O_{5.5}$ | | | 854 | | 706 | 582 |

[a] IR spectra recorded in diffuse reflectance mode on samples mixed with KBr.

resulting in a loss of the $Ag^+$−O interaction in the lattice, moving the V=O stretching frequency closer to the value observed in $V_2O_5$. Past 1.2 equiv of Li the V=O bands display a red shift down to 854 $cm^{-1}$ for $Li_{3.3}AgV_2O_{5.5}$. This shift is consistent with the reduction of $V^{5+}$ to $V^{4+}$ in this discharge range, where $V^{4+}$=O would be expected to display a lower stretching frequency than $V^{5+}$=O. Vanadium(III) oxides, such as $V_2O_3$, give rise to poorly defined spectra,[27] which suggests that this species is not observable in the FT-IR spectra.

The voltammetric behavior of SVO has been described in detail elsewhere.[10] The reduction consists of four major waves between 3200 and 1700 mV as illustrated in the voltammogram of Li/SVO in Figure 8. The waves in the range 3200−2750 mV were assigned to the reduction of $V^{5+}$ and $Ag^+$. The remaining waves at 2550 and 2000 mV were assigned to $V^{5+} \rightarrow V^{4+}$ and $V^{4+} \rightarrow V^{3+}$ reductions, respectively. It should be noted that while the voltammogram in Figure 8 displayed well resolved reduction waves, it was acquired using a slow scan rate of 0.08 mV/s. Voltammograms of Li/SVO acquired at higher scan rates, more similar to the rate of discharge utilized in the constant resistance discharge experiments, display greater overlap of peaks. The overlap of $V^{5+}$ and $Ag^+$ reduction waves in the range of 3200 to 2750 mV is consistent with the simultaneous formation of $V^{4+}$ and $Ag^0$ for $x < 1.2$, assigned via the physical characterization studies.

The large peak current for the wave assigned to $V^{5+} \rightarrow V^{4+}$ reduction at 2550 mV in Figure 8 suggests that the majority of the vanadium(V) was reduced at this potential. The separation

(28) Hui-Liang, Z.; Wei, Z.; Xiang, D.; Xian-Cai, F. *J. Catalysis* **1991**, *129*, 426.
(29) Arof, A. K.; Radhakrishna, S. *JALCOMP* **1993**, *200*, 129.
(30) Fikis, D. V.; Heckley, K. W.; Murphy, W. J.; Ross, R. A. *Can. J. Chem.* **1978**, *56*, 3078.

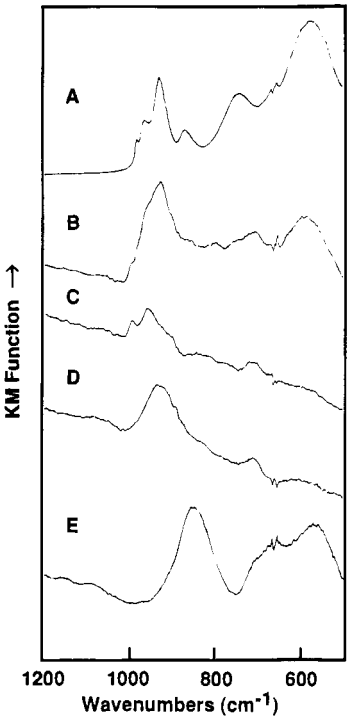


**Figure 7.** FT-IR diffuse reflectance spectra of SVO and discharged SVO samples: (A) $AgV_2O_{5.5}$; (B) $Li_{0.35}AgV_2O_{5.5}$; (C) $Li_{1.2}AgV_2O_{5.5}$; (D) $Li_{1.9}AgV_2O_{5.5}$; (E) $Li_{3.3}AgV_2O_{5.5}$ mixed with KBr.

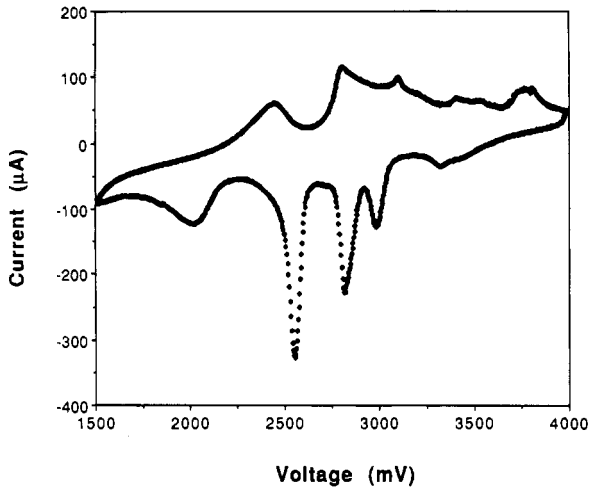


**Figure 8.** Voltammogram of SVO vs Li at a scan rate of 0.08 mV/s in 1 M $LiAsF_6$ propylene carbonate/dimethoxyethane electrolyte.

between this wave and the $V^{5+} \rightarrow V^{4+}$ wave in the 3200−2750 mV range suggests that the electronic environments surrounding the respective $V^{5+}$ centers are significantly different. In addition, these waves occur at voltages corresponding to plateaus at $0 < x < 0.8$ and $1.5 < x < 2.3$ in the voltage profile for the Li/SVO discharge reaction (Figure 1), and at slower rates of discharge these plateaus are more well defined.[10] A plateau in a coulometric titration curve indicates that at least two phases are present in equilibrium, while sloping cell voltage corresponds to a single phase region.[31] The observation of plateaus in these regions of the curve suggests that vanadium(V) reduction results in the formation of new phases of $Li_xAgV_2O_{5.5}$.

(31) Crouch-Baker, S.; Huang, C.-K.; Huggins, R. A. In *Proceedings of the Symposium on Primary and Secondary Ambient Temperature Lithium Batteries*; Gabano, J. P., Takehara, Z., Bro, P., Eds.; The Electrochemical Society: Pennington, NJ, 1988; Vol. 88-6; p 44.

## Conclusions

The incorporation of lithium cations into the open framework of SVO during the electrochemical Li/SVO reaction is accompanied by a reduction of the SVO material. Thus, the SVO cathode material is transformed both chemically and electrochemically by the reduction reaction that takes place in lithium batteries. By using a diverse set of solid-state characterization techniques, structural and electronic changes were identified in the lithiated SVO products. Structural changes in the material were evident upon discharging SVO to $Li_xAgV_2O_{5.5}$ ($0 < x < 1.2$). A loss of peaks due to crystalline $\epsilon$-phase SVO from the X-ray powder pattern suggests that intercalation of lithium causes disorder in the structure of SVO. This is consistent with the FT-IR results for the discharged samples, where bands assigned to the V−O−V backbone of SVO disappear upon lithiation of the sample. However, although the majority of the starting SVO peaks in the XRPD pattern decrease in intensity during the discharge reaction, the 001 peak is still observed to the deepest depth of discharge ($x = 3.3$). A decrease in the $d_{001}$ spacing seen in these powder patterns, coupled with the observed swelling of the cathode materials with discharge suggests that the other unit cell parameters increase to accommodate the change in cell volume. The structural implications are that the observed contraction of the $c$ lattice parameter with lithiation moves the $VO_x$ units closer together within the same layer, while inferred expansion of the $b$ lattice parameter would widen the channel between layers to accommodate the incorporation of lithium. This proposal is consistent with the changes seen in structure of $V_2O_5$ with lithiation.

Electronic changes were also observed for the discharged SVO samples. The formation of elemental silver was identified by X-ray diffraction. The reduction of silver in the Li/SVO reaction is important, since it accounts for ~30% of the overall capacity of the cathode material and improves the conductivity of the material. Furthermore, these results indicate that the $Ag^+ \rightarrow Ag^0$ reduction takes place early in the discharge reaction ($0 < x < 1.2$), but only accounts for ~75% of the observed cell capacity in this range. This suggests that a simultaneous reduction of vanadium(V) must occur to fill out the balance of the cell capacity. This conclusion is consistent with the voltammetry of Li/SVO, where the silver reduction wave in the voltammogram overlaps with a vanadium reduction wave. The identification of $Ag^0$ in the sample by XRPD suggests that the material may be described as a mixture of $LiV_2O_{5.5} + Ag^0$ at the $x \sim 1$ point. Thus the lithiated vanadium oxide formed in SVO would be similar in composition to the product of $V_2O_5$ lithiation. However, the discharge curves for SVO and $V_2O_5$ are significantly different. In the lithiation of $V_2O_5$ two plateaus are observed in the range of $0 < x < 1$ for $Li_xV_2O_5$, at voltages of ~3.4 and 3.3 V vs $Li/Li^+$.[20,32] These voltages are significantly higher than those seen for the lithiation of SVO (Figure 1). Additionally, the $V_2O_5$ discharge curve displays a sharp drop in voltage at $x = 1$, followed by a plateau at ~2.3 V. This plateau occurs at a lower voltage than the corresponding section of the Li/SVO discharge curve. The differences in the discharge curves for these species suggests that lithiated vanadium oxide produced by the discharge of SVO is structurally distinct from the material produced by the lithiation of $V_2O_5$.

As the discharge reaction proceeds past the $x = 1.2$ point, the electrochemical activity switches from silver to vanadium reduction. This is consistent with the FT-IR spectra of the SVO samples in this discharge range, where a substantial red shift

(32) Gourier, D.; Tranchant, A.; Baffier, N.; Messina, R. *Electrochim. Acta* **1992**, *37*, 2755.

of the V=O stretching frequency correlates with the reduction of $V^{5+}$ to $V^{4+}$. Likewise, a large increase in room temperature magnetic susceptibility for $x > 1.2$ suggests the formation of paramagnetic reduced vanadium. On the basis of chemical analysis of the products of the lithiation reaction in the range of $1.2 < x < 1.9$, the reaction results exclusively in the reduction of $V^{5+}$ to $V^{4+}$, which is in agreement with the voltammetry results. Furthermore, a phase change in the material is suggested by the appearance of a plateau in the discharge curve, which is consistent with the DSC analyses of the samples. As the reduction of SVO continues past $x = 1.9$, a mixture of oxidation states for the vanadium components is observed. The reduction of $V^{4+}$ to $V^{3+}$ competes with the reduction of the remaining $V^{5+}$ to $V^{4+}$, resulting in the formation of mixed-valent materials, where vanadium(V), -(IV), and -(III) are found in the same sample.